COMBINING HIGH-FIDELITY HELICAL MICRO-TOMOGRAPHY WITH REGION-OF-INTEREST SCANNING FOR IMPROVED CORE CHARACTERISATION

Trond K. Varslot, Andrew M. Kingston, Shane J. Latham, Jill Middleton,
Mark A. Knackstedt and Adrian P. Sheppard
Department of Applied Mathematics, Australian National University, Canberra, Australia

This paper was prepared for presentation at the International Symposium of the Society of Core Analysts held in Austin, Texas, USA 18-21 September, 2011

ABSTRACT

Digital imaging of core material and subsequent computational analysis of petrophysical and multiphase flow properties is gaining popularity as a method to characterize reservoir core material at multiple scales. Particular interest in the technology is focused on applications where traditional core analysis is more uncertain and imaging at multiple scales is required (e.g. tight gas and carbonate reservoirs) or core is difficult to work with (unconsolidated sands). In this paper we describe novel scanning technology which greatly enhances the ability to characterize these problematic classes of core material.

A new helical trajectory X-ray micro-CT instrument that enables high-resolution (micro/nano) tomography with a higher signal-to-noise ratio (SNR) is described. Helical scanning provides several advantages over the standard circular scanning systems: exact reconstruction methods, faster data collection and the ability to image core of arbitrary length. The design allows scanning of samples at multiple scales (whole core to sub micron scales) on a single hardware system at a range of resolutions. Case studies describing the imaging and coupling of image data from heterogeneous coal samples, carbonate core material and tight gas reservoirs at plug to micropore scale are presented.

We also describe recent advances in region-of-interest (ROI) tomography which allow one to generate high-resolution artifact-free images of small subregions of larger samples without the need for physical subsampling. This approach is particularly beneficial for the analysis of poorly consolidated core materials that cannot be cored without disturbance to a sufficiently small size for full pore-space characterisation without disturbance. To illustrate we present results for an unconsolidated material cored to 38mm, for which standard imaging yields images of 28μm voxel size; too coarse for modelling petrophysical properties of interest. We show images from the interior of the sample with a voxel size of 10μm that is sufficient to capture the structure of interest.

INTRODUCTION

The emergence, over the last decade, of commercial laboratory X-ray micro-CT (MCT) instruments that can acquire high quality 3D images of rock core samples on the micron scale has attracted a great deal of attention. In particular, the now proven ability of X-ray micro-CT imaging to capture the essential features of the pore space of cleaner reservoir samples [13] means that it is being rapidly adopted around the world. However, the industrial benefit of a new analysis technique for straightforward samples is limited since reservoirs containing such rocks are typically well understood already. The utility of MCT technology depends more, therefore, on its ability to make contributions to the characterisation of more difficult samples, often from unconventional fields, where traditional techniques may have left significant uncertainties. In this work we will consider some samples where we believe that MCT can make particular contributions, namely to heterogeneous coals, tight gas sands and unconsolidated materials.

The primary difficulty that one faces when imaging tight or heterogeneous samples is the range of length scales that must be considered. This is of particular severity in 3D imaging since the image size grows with the cube of the side length. For example, in many carbonates or tight gas sands, there are important features only tens of nanometers in size, while any piece less than 10mm in size has little hope of being representative. A cubic image capturing this data would therefore need one million voxels on each side, resulting in an image containing 10^{18} voxels, close to a billion times larger than could be acquired or processed today.

Consequently, one must compromise when undertaking MCT studies of all but the most straightforward samples. In this article we present two new techniques that help to improve this compromise. The first is helical scanning, that yields low noise, higher-fidelity images and that allows one to image long thin pieces of core in reasonable acquisition time. The second is region-of-interest (ROI) imaging, also called interior tomography, which enables one to image a subvolume from within a sample, alleviating the need to cut a sample to fit completely within the field of view.

HELICAL SCANNING TOMOGRAPHY

Tomographic imaging at a laboratory MCT facility involves the use of a point X-ray source, which results in a cone-beam geometry. In such a geometry, the circular scanning trajectory that results from simply rotating the sample does not provide complete information about the object, with the information deficiency growing as one gets further from the system's optical axis, i.e. as the angle of divergence of the beam grows. Cone-beam reconstruction methods [11] from circular scanning are therefore approximations only. The practical consequence of this is that one is restricted to a *cone angle* of about 10°, limiting how close the camera can be placed to the source, and even at this angle some geometries will be poorly reconstructed. This cone angle restriction is most unfortunate, since the Bremsstrahlung X-ray sources used in laboratory systems give off X-rays over almost a full hemisphere, meaning that about 99% of the X-rays are wasted if the cone angle is 10°. Since the flux given off by such sources is limited by

basic physics (the target material is vaporised if the flux is too high), and since MCT is quantum limited (i.e. image noise is determined by detector shot noise), long acquisition times are invariably used to avoid poor image quality.

It has been known for 20 years [12] that helical scanning trajectories, where the sample is translated vertically (along the rotation axis) during rotation, provide sufficient information about the sample and therefore admit exact reconstruction methods. However, it turned out to be extremely difficult to devise an exact method for helical tomographic reconstruction that was both accurate and practical to implement. It was not until the landmark work of Katsevich in 2002 [10] that an exact inversion formula of the filtered backprojection type was found. The Katsevich formula has the additional advantage that only horizontal or nearly-horizontal filtering is required, allowing one to scan objects of arbitrary length without resorting to image stitching.

In the context of MCT, Katsevich reconstruction is difficult to implement since it places higher demands on the hardware alignment, particularly that the source-sample distance must be known to micron precision, and that the angle between the translation direction and the rotation axis must be constant and known. This is troublesome since the X-ray source point is located at a depth of at least 500μm inside the X-ray tube, and can move as the filament or target degrade during normal use. To our knowledge, we are the first to have implemented Katsevich for MCT, and use a novel software-based "autofocus" alignment method [2] to eliminate the need for perfect hardware alignment. We are now routinely imaging with a cone angle of 40°, which means that we are capturing nearly 20% of the X-ray beam. This has resulted in an order-of-magnitude improvement in image acquisition time for the same image quality, or the ability to image long cores or capture higher quality images within reasonable times [7].

Tight Gas Sand Sample

An imaging study was undertaken on a heterogeneous, laminated tight gas sand sample of 7% porosity and 0.03mD permeability. Initial quick scanning of a 38mm core suggested that the material was too heterogeneous to image at our usual sample size of 5mm (see Figure 1). However, the sample's low permeability, along with thin section and capillary pressure data (Figures 2 and 3) showed that sub-micron resolution would be required to capture the key details of the pore space. An additional difficulty was that the less well cemented regions were already somewhat fractured and had little mechanical integrity. To achieve the best balance between resolution and field of view, a 38×9mm core of square cross-section was taken perpendicular to the bedding plane, as shown in Figure 1.

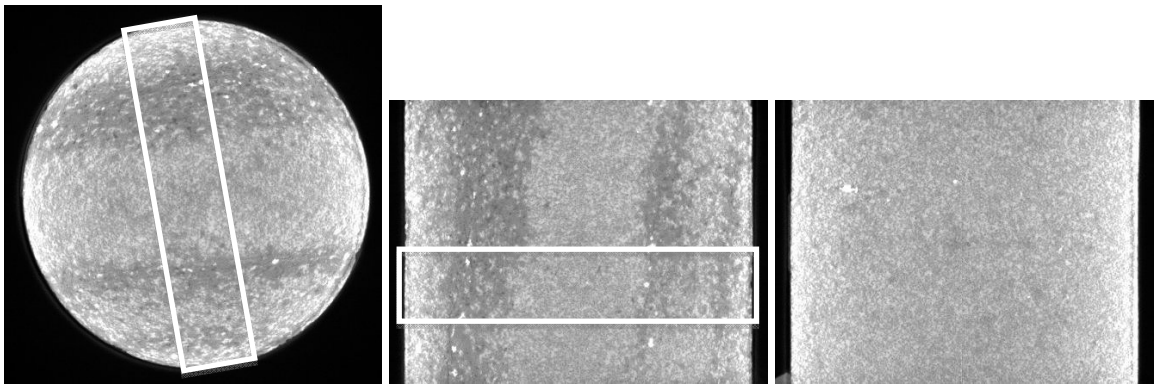

Figure 1: Initial MCT image of three othogonal slices through the full core of the tight gas sand, showing laminations and relative homogeneity parallel to the laminations. Superimposed rectangles indicate size and orientation of the prismatic core shown in Figures 4 and 5. Significant beam hardening is evident.

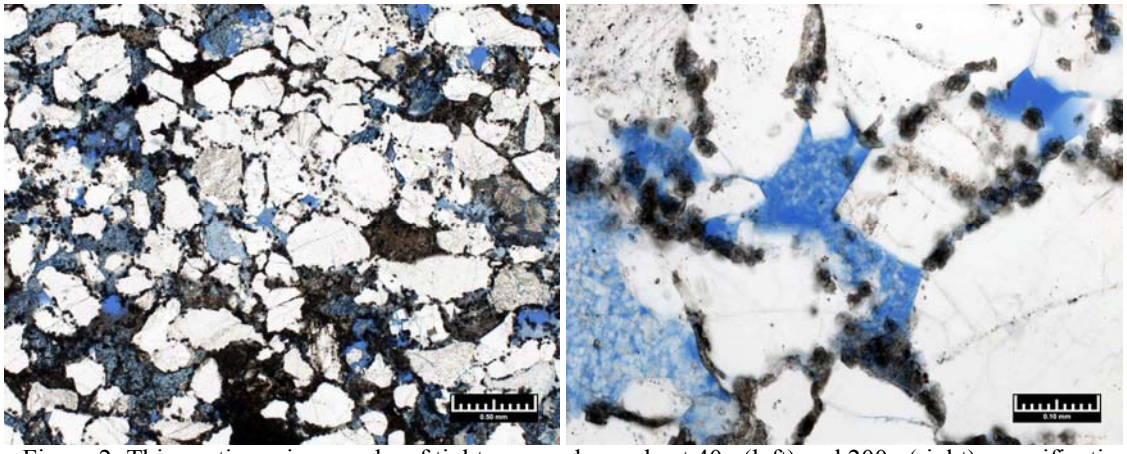

Figure 2: Thin section micrographs of tight gas sand sample at 40x (left) and 200x (right) magnification.

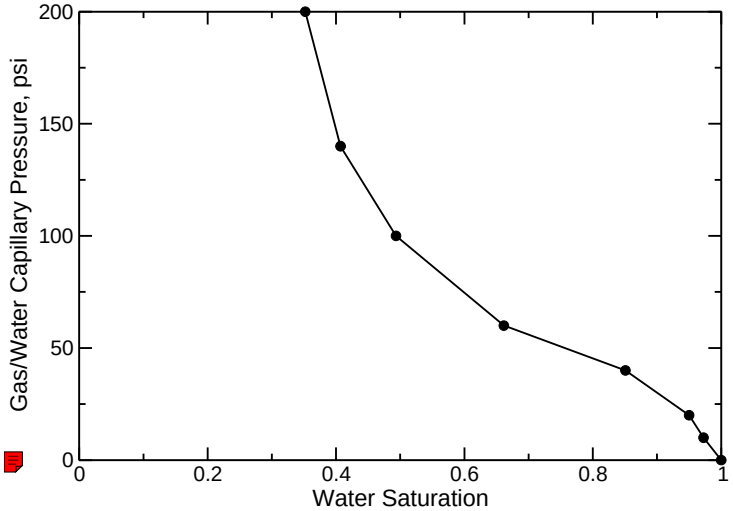

Figure 3: Gas-water capillary pressure for the tight gas sand sample.

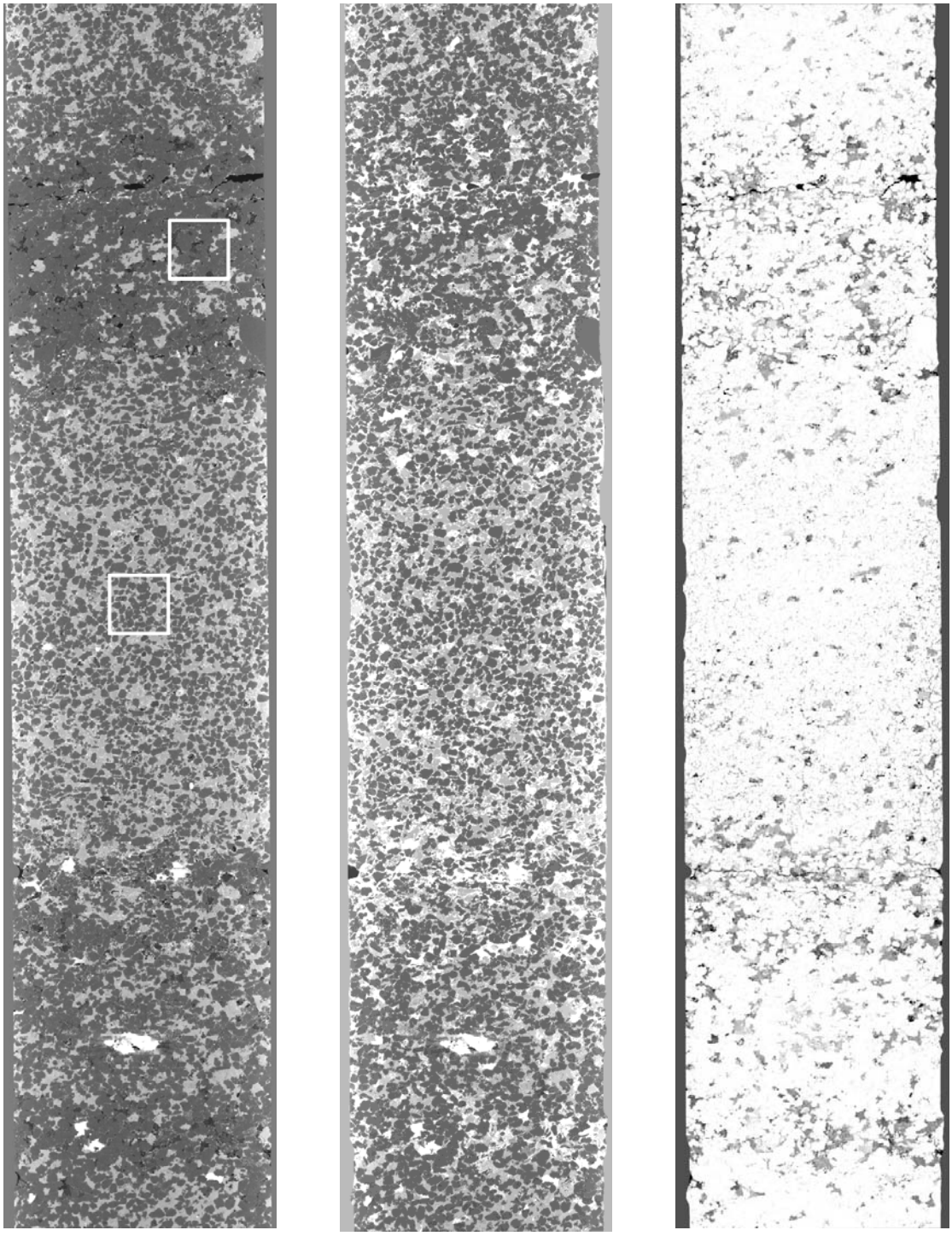

(a) (b) (c)

Figure 4: Helical MCT images of prismatic 9mm core of tight gas sand, showing (a) dry sample, (b) sample saturated with 1M CsI and (c) linear grayscale porosity map calculated by image subtraction (black=100% porous, white=100% nonporous). Images are 1400×6200 pixels of 5.9μm, field of view 8.2×36.5mm. Two fractures in less cemented regions are visible in (c); the upper fracture was disturbed during sample preparation and some grains were lost. White squares on (a) show the location of images in Figure 5.

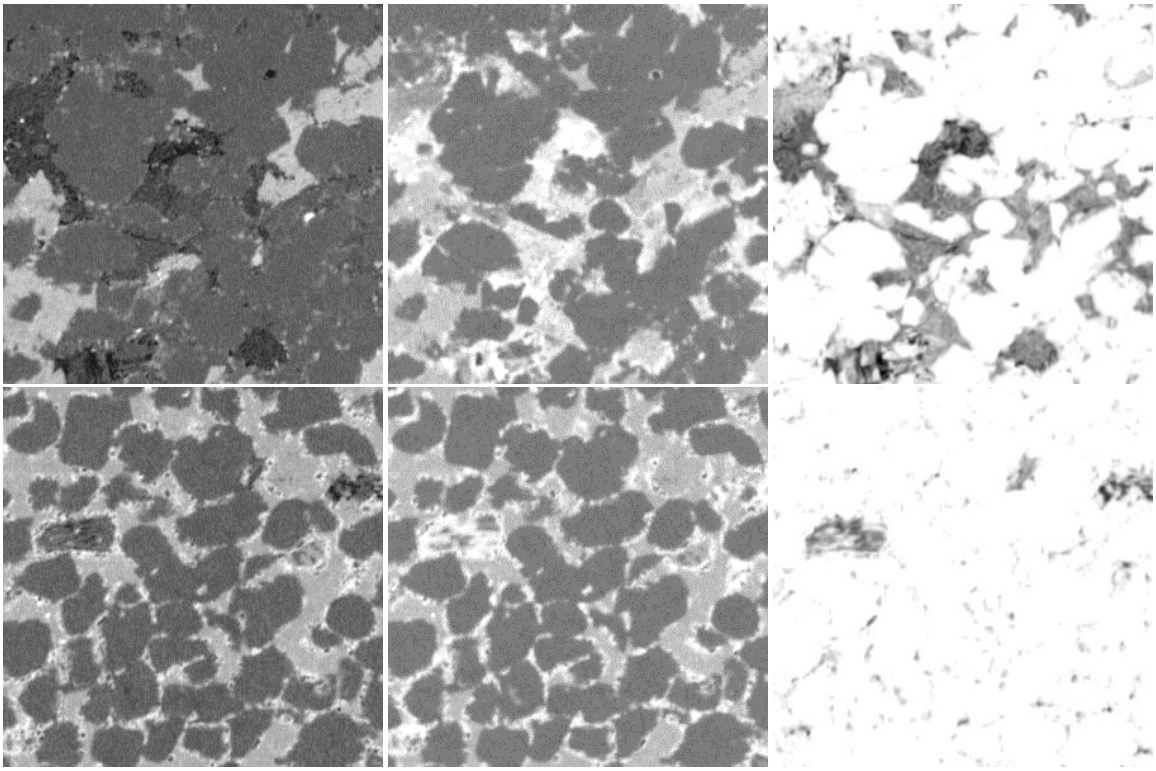

(a) **(b)** **(c)**

Figure 5: Zoom into the two locations indicated by the squares overlaid on Figure 4(a). Top: less cemented, more clay rich region, showing some siderite precipitation. Bottom: region heavily cemented with ankerite. As for figure 4, (a) show dry sample, (b) saturated sample and (c) porosity map. Images are 300^2 pixels giving a field of view of 1.75×1.75mm in all images.

Figures 4 and 5 illustrate the imaging that's been performed on the prismatic piece, which was imaged both dry and in a saturated state, with the resulting images then registered [3]. Several things should be noted from these images. First is that our procedure for saturating the sample was imperfect and left behind some air bubbles. This can be observed in the top middle image in Figure 5. The bubbles seem to be located in the most open regions, which is consistent with capillary trapping, and indicate that an improved procedure is needed for tight samples like this - the current method involves placing the sample in degassed water then leaving it for 24-48 hours under a vacuum. In this case, the bubbles are sufficiently isolated that they should not significantly affect our results. The second noteworthy point is that the tiny pores inside the siderite nodules are not saturated with the imbibing fluid, showing that these regions are genuinely inaccessible.

Due to the tight nature of the sample, and the moderate resolution of these images, the pore space geometry is not captured in enough detail to directly model properties such as permeability. Nevertheless, some properties can be calculated from a *porosity map* as shown on the right of Figures 4 and 5. This map assigns a microporous fraction to each

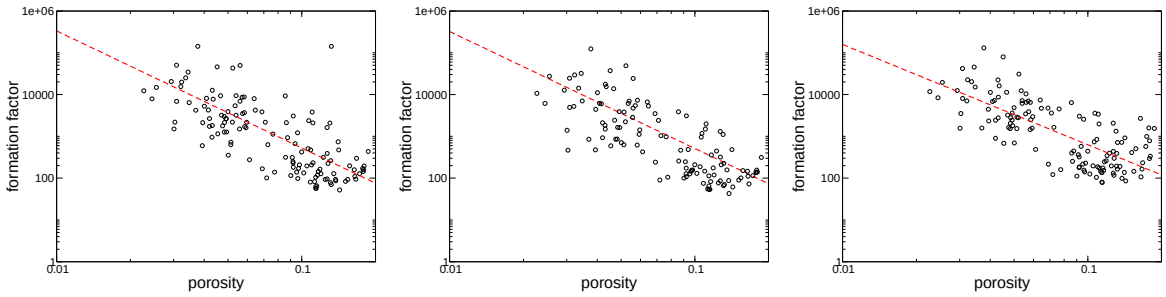

Figure 6: Formation factor vs porosity for the tight gas sand, in the X, Y and Z directions left to right, where Z is normal to the bedding plane. Each data point represents a calculation on a 300^3, 1.75mm cubic subvolume. The linear fit yields cementation exponent m=2.8 for X and Y, 2.4 in the Z direction. These values are larger than the measured value of m=2.1 which was obtained at a much larger scale.

image voxel, and can only be calculated from a subtraction of the dry from the wet image. The porosity map provides sufficient information to calculate the formation factor; we do this on many 300^3 (1.75mm cube) subvolumes to estimate the cementation exponent (see Figure 6).

Fractured Coal Sample

With the advent of coal seam gas (or coalbed methane), the structure of the pore space of coal is now attracting a great deal of interest. Coal is difficult for MCT analysis for a number of reasons. Firstly, the material itself provides relatively poor X-ray contrast, yet often contains highly attenuating inclusions. Secondly, it invariably contains both large fracture networks and sub-micron porosity, the connectivity of which must be described in order to model transport properties. By combining helical imaging and wet/dry image registration we have been able to answer many important questions. Figure 7 shows slice images of a banded bituminous coal from the Western Sydney Basin, NSW, Australia. A combination of the wet and the dry images enables one to map both the fracture network and the microporosity, laying a foundation for the calculation of further physical properties.

REGION OF INTEREST IMAGING

MCT is a non-destructive imaging modality. However, specimens must be sectioned or cored to enable the imaging of specific regions at a sufficient resolution. Sectioning is not feasible in many instances due to sample uniqueness or fragility. Another consideration is that the act of sectioning or coring a specimen may change its properties near the boundary. Region-of-interest (ROI) tomography is therefore of great potential value. Naïve attempts at ROI imaging result in cupping artifacts where the material appears brighter at the edge, while mathematically speaking, ROI tomographic reconstruction has no unique solution. The problem of inversion from interior projection data was first considered over thirty years ago [9]. There are several approaches to overcome the lack of global knowledge: (a) reconstruct a localised function, e.g. the sample gradient rather than the attenuation itself [14]; (b) regularise the problem using *a priori* knowledge of the

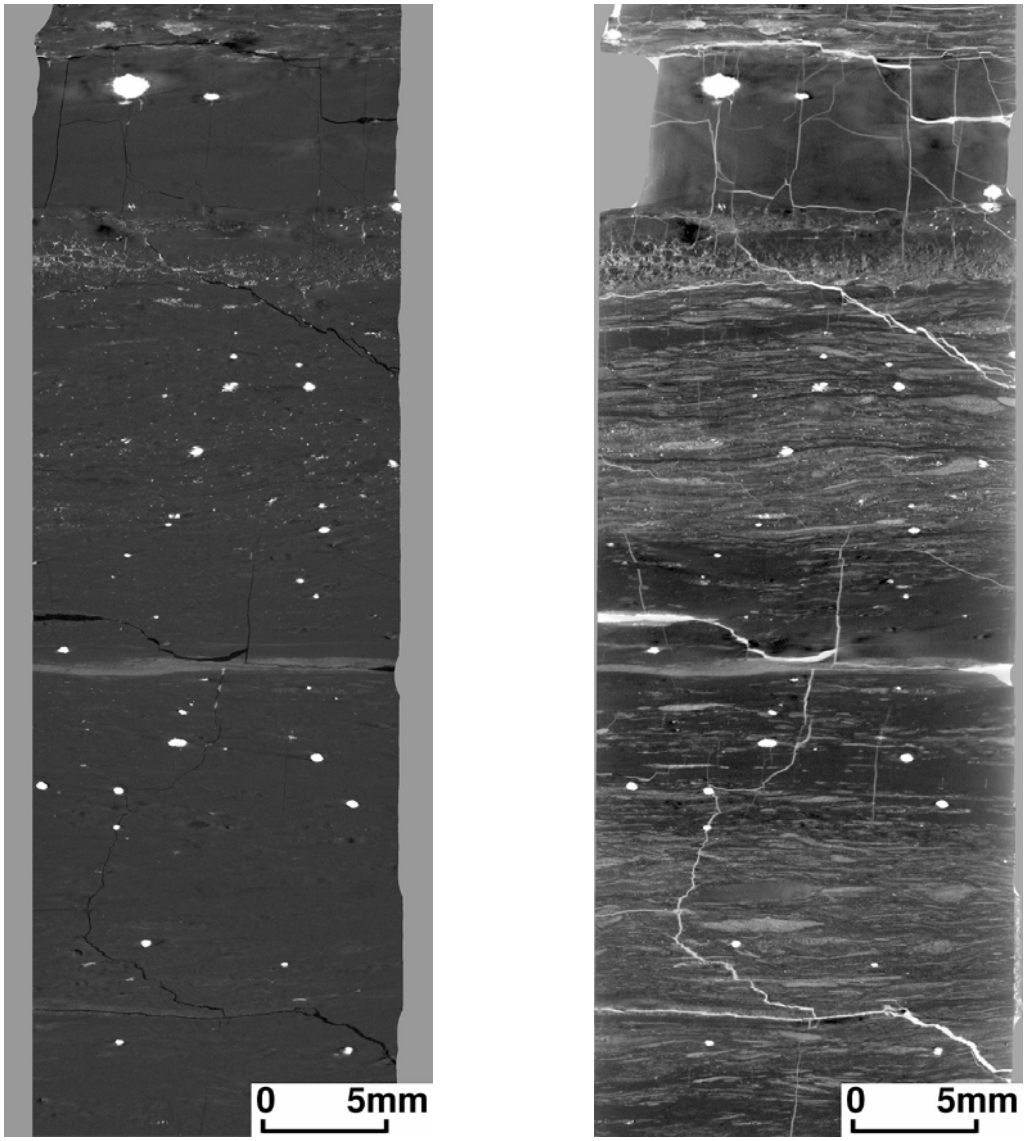

(a) (b)

Figure 7: Registered slice images of coal sample. The dry sample is shown at left; the right image shows the sample after saturation with an aqueous 1M CsI solution, which has revealed microporosity that was invisible in the original image. The white nodules are most likely siderite. The vertically fractured bands of coal are vitrite and the microporous and mineralised bands of coal are inertite.

sample [8]; (c) localise the reconstruction operation, (or Radon transform) in the wavelet domain [1, 5, 6]; or (d) extrapolate the projection data [4].

In this work we use the method of projection data extrapolation. Natterer [4] showed that, up to an additive constant, a reasonable extrapolation of the projection data into the unknown regions suffices to recover an *accurate* approximation of the sample. Since our objective here is to obtain a segmentable image, we are not concerned with an additive constant. This method is implemented with a single change to the ramp-filtering

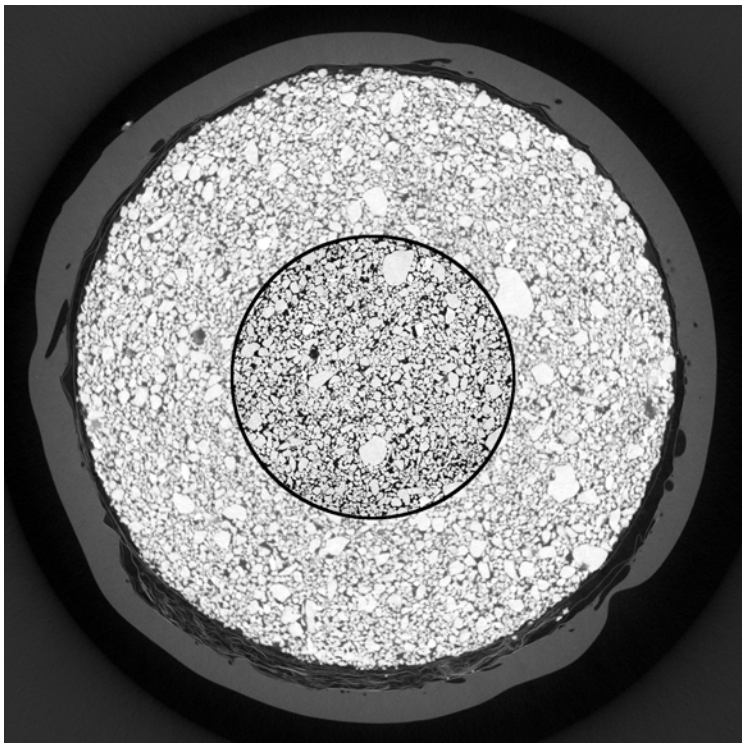

Figure 8: Cross section of the sand sample showing the 20mm diameter ROI on the full sleeved 38mm core

step in reconstruction and does not require time consuming iterations or any additional data, such as global projections. Because the method is based upon extrapolation of projection data it works best for homogeneous materials and at this time is only usable on cylindrical samples. Essentially we model the projection of a rock core as that of a uniform cylinder and then determine the best cylinder parameters that fit the measured ROI projections. We use this model to extrapolate each row in the projections from a field-of-view of N pixels out to 2N pixels. Our results agree with Natterer: the relative attenuations are correct but an additive constant is introduced.

Unconsolidated Sand Sample

A poorly consolidated sand sample (shown in Figure 8) was received as a 38mm core in a thick wax sleeve, the removal of which risked disturbing the core. Standard imaging, needing some clear space on both sides of the sample, demanded a 54mm field of view, resulting in a voxel size of 28μm. A helical ROI scan was then performed on a 20mm diameter cylinder in the centre of the core (Figure 8), allowing a 10.2μm voxel size. The two images were registered (aligned) and close-up images are shown in figure 9, from which a striking improvement in image quality is clear. Figure 10 shows grey-value histograms of the two images; the unsatisfactory unimodal distribution of the original image is transformed into a clear bimodal distribution in the ROI scan. The clarity of the image and the obviously bimodal histogram indicate that the ROI scan is of sufficient quality and resolution to allow segmentation and petrophysical modelling.

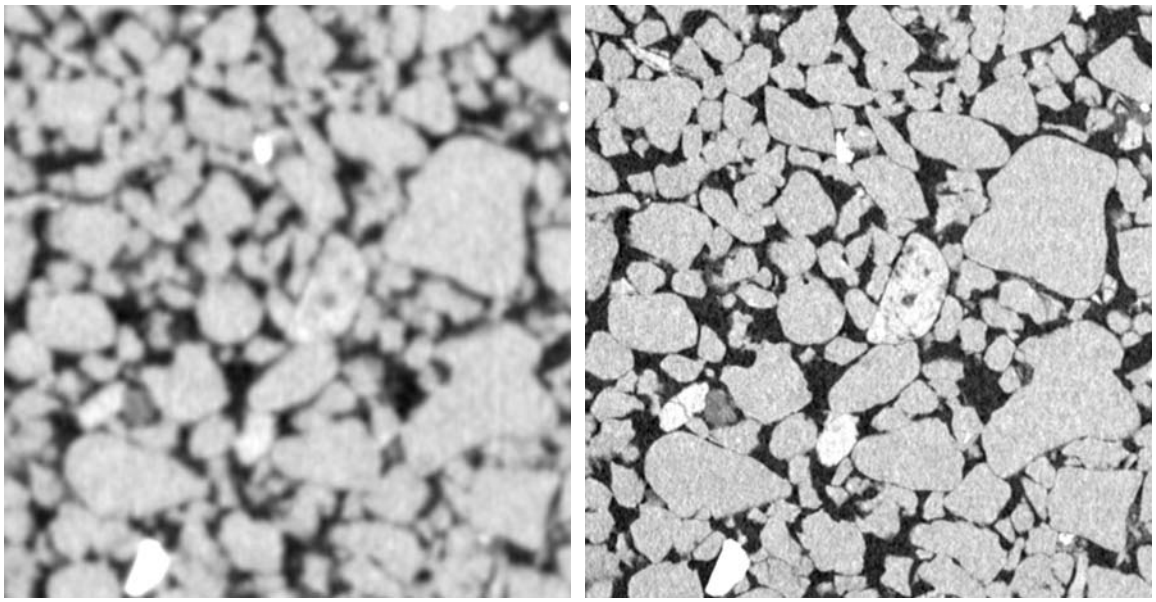

Figure 9: Close-up from figure 8, comparing standard image of 38mm unconsolidated sand (left) with higher resolution region of interest scan (right). ROI scan has 20mm field of view and 10.2µm voxel size, versus original scan with 54mm FOV (including sleeve and clear space on edges) and 28µm voxel size. The ROI scan captures the pore space geometry in sufficient detail to allow petrophysical analysis, whereas the original image is inadequate. Acquisition time for both images is 20 hours.

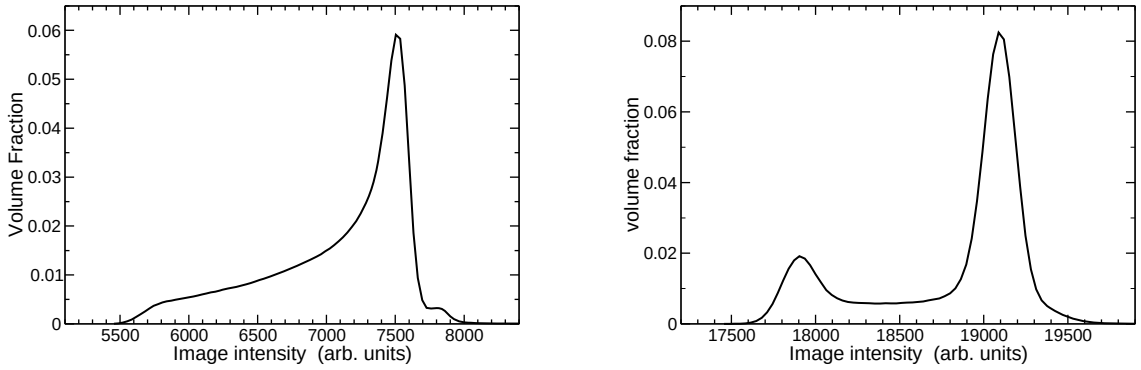

Figure 10: Histogram of image grayscale values obtained for the original image (left) and region of interest scan (right), i.e. from the images shown in Figure 9. The small and large peaks in the ROI histogram correspond to air and quartz respectively.

Tight Gas Sand Sample

The fact that ROI scanning can capture a very long and thin image without requiring the sample to be cored into that shape is of particular value when considering laminated sands such as the tight gas sand shown earlier. Due to weaknesses in the less cemented regions it was impossible to take a sufficiently small diameter core while also approaching a representative length across the laminations. We were, however, able to take a higher resolution ROI scan on the inner 5mm of a cylindrical 8mm core that lies

adjacent to the 9mm prismatic sample used in the previous section. The new scan had 2.4μm voxel size and a total height of 13mm, although a much longer region could have been captured if time had permitted. Figure 11 is shows close-ups from a standard image on the prismatic sample and from the ROI image. Even though these are not registered images of the same region, it is clear that the ROI scan has captured many details of the pore space, particularly the pore filling kaolinite, that are unclear in the original image.

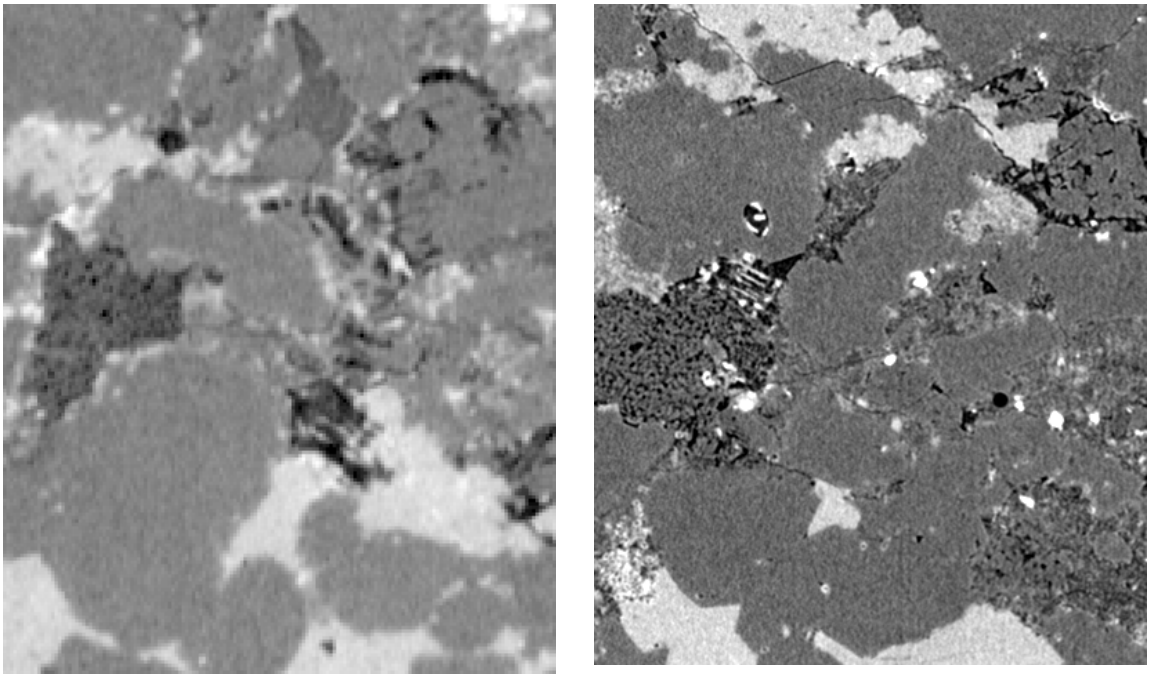

Figure 11: Close-up slice images of the tight gas sand, comparing standard image (left, 5.9μm voxel size) with higher resolution ROI scan (right, 2.4μm voxel size) of a sister sample. The area shown in both images is 1.15×0.96mm.

CONCLUSION

We have demonstrated two new technologies for the imaging of rock core samples: helical scanning and region-of-interest (ROI) scanning. Helical scanning allows one to capture a very high solid angle of X-rays from the source, allowing high quality images of samples of arbitrary length. When combined with ROI scanning, one can take images of long thin samples that capture 3D information across length scales that was not previously feasible. When used together and combined with 3D registration, this represents a powerful approach for improved characterisation of problematic core.

ACKNOWLEDGEMENTS

We acknowledge the financial support of the member companies of the ANU/UNSW Digital Core Consortium, and to the Australian Research Council who provided funding through grants DP110102964 and FT100100470.

We are grateful to ConocoPhillips for provision of core material, related information and helpful discussions and also to DigitalCore Pty Ltd, particularly Alexandra Golab, for providing both data and advice. Thanks also to Benjamin Young and Michael Turner for sample preparation and imaging.

REFERENCES

1. A. Delaney and Y. Bresler, "Multiresolution Tomographic Reconstruction using Wavelets," *IEEE Transactions on Image Processing*, vol. **4**, no. 6, p. 799–813, 1995.
2. A. M. Kingston, A. Sakellariou, A. P. Sheppard, T. K. Varslot, and S. J. Latham, "An auto-focus method for generating sharp 3D tomographic images," in *Proceedings of SPIE*, 2010, vol. **7804**, p. 78040J.
3. S. Latham, T. Varslot, and A. Sheppard, "Image Registration: enhancing and calibrating X-ray micro-CT imaging," in *22nd International Symposium of the Society of Core Analysts*, Abu Dhabi, UAE, 2008.
4. F. Natterer, *The mathematics of computerized tomography*. New York: Wiley, 1986.
5. T. Olson and J. Destefano, "Wavelet Localization of the Radon Transform," *IEEE Transactions on Signal Processing*, vol. **42**, no. 8, p. 2055–2067, 1994.
6. F. Rashid-Farrokhi, K. Liu, C. Berenstein, and D. Walnut, "Wavelet-based multiresolution local tomography," *IEEE Transactions on Image Processing*, vol. **6**, no. 10, p. 1412–1430, 1997.
7. T. Varslot, A. Kingston, A. Sheppard, and A. Sakellariou, "Fast high-resolution micro-CT with exact reconstruction methods," in *Proceedings of SPIE*, 2010, vol. **7804**, p. 780413.
8. J. Yang, H. Yu, M. Jiang, and G. Wang, "High-order total variation minimization for interior tomography," *Inverse Problems*, vol. **26**, no. 3, p. 035013, 2010.
9. C. Hamaker, K. Smith, D. Solmon, and S. Wagner, "The divergent beam x-ray transform," *Rocky Mountain Journal of Mathematics*, vol. 10, pp. 253–283, 1980.
10. A. Katsevich, "Theoretically exact filtered backprojection-type inversion algorithm for spiral CT," *SIAM Journal on Applied Mathematics*, p. 2012–2026, 2002.
11. L. Feldkamp, L. Davis, and J. Kress, "Practical cone-beam algorithm," *J Opt Soc Am*, p. 612–619, 1984.
12. H. K. Tuy, "An inverse formula for cone-beam reconstruction," *SIAM J Appl. Math.*, vol. **43**, p. 546–552, 1983.
13. C. Caubit, G. Hamon, A P. Sheppard, and P. E. Ören, "Evaluation of the reliability of prediction of petrophysical data through imagery and pore network modelling," in *22nd International Symposium of the Society of Core Analysts*, Abu Dhabi, UAE, 2008.
14. K. Smith, "Inversion of the X-Ray Transform," in *Proc. SIAM-AMS*, 1984, vol. 14, p. 41.